AiCARR Journal / Vol 63, n. 4, 56 - 63, 2020

Marco Noro[1]*, Simone Mancin[1], Renato Lazzarin[1], Giulia Righetti[1]

Energy performance and economic viability of enhanced hybrid PCM thermal storages using aluminum foams for solar heating and cooling

Prestazioni energetiche e fattibilità economica degli accumuli termici ibridi con materiali a cambiamento di fase incentivati con schiume di alluminio per il riscaldamento e il raffreddamento solare

[1] Department of Management and Engineering, University of Padova, Vicenza, Italy

***Corresponding author:**
Marco Noro
Department of Management and Engineering
University of Padova
Stradella S. Nicola 3
36100 Vicenza, Italy
marco.noro@unipd.it
tel +39 0444 998704

DOI: 10.36164/AiCARRJ.63.04.04

Abstract

Considerable advantages can be achieved in solar heating and cooling plants by improving the energy storage capabilities of hybrid water thermal energy storage by using phase change materials (PCMs). However, the most suitable materials find intrinsic limitations due to their poor heat transfer capabilities. This paper depicts the simulation work, based on experimental measurements, of enhanced hybrid sensible-latent water thermal energy storages using aluminum foams as heat transfer medium to improve the overall heat transfer of the PCM. The annual performance of a solar heating/cooling and ground source absorption heat pump plant in northern Italy are evaluated by Trnsys. The dynamic simulations allow to define the best configuration of the plant from both energy and economic point of view considering different cases: all three tanks modeled as sensible (water) storage, or one of the tanks modeled as PCM storage, or as enhanced PCM with metal foam.

Keywords:

- Hybrid thermal energy storage
- PCM
- Metal foam
- Dual source heat pump
- Ground source heat pump

Sommario

L'utilizzo di materiali a cambiamento di fase (phase change materials, PCMs) negli accumuli termici ibridi (acqua-PCM) consente vantaggi notevoli nei sistemi di riscaldamento e raffrescamento solari. Tuttavia, i materiali maggiormente adatti trovano delle limitazioni intrinseche dovute alla loro bassa conduttività termica. Questo articolo descrive il lavoro di modellazione/simulazione, basato su misure sperimentali, dell'utilizzo di accumuli termici ibridi acqua-materiali a cambiamento di fase incentivati con schiume di alluminio, al fine di incrementare la capacità di scambio termico. Vengono analizzate tramite software Trnsys le prestazioni di un impianto solare di riscaldamento e raffrescamento accoppiato con pompa di calore a terreno in un edificio a uso palestra ristrutturato nel nord Italia. Le simulazioni dinamiche consentono di definire la configurazione migliore dal punto di vista sia delle prestazioni energetiche che dell'analisi economica tra i diversi casi considerati: tutti e tre i serbatoi modellizzati di tipo sensibile (acqua), oppure uno dei serbatoi di tipo PCM, oppure un serbatoio PCM incentivato con schiuma metallica.

Parole chiave:

- Accumulo termico ibrido
- Materiale a cambiamento di fase
- Schiuma metallica
- Pompa di calore a doppia sorgente
- Pompa di calore a terreno

Introduction

Sensible (water) Thermal Energy Storages (TESs) are widely diffused in heating and cooling plants. As a drawback, they require relevant volumes per unit of stored energy according to the acceptable temperature difference ΔT (4.187×ΔT MJ m^{-3}, that is 0.86×ΔT m^3 kWh^{-1}). A reduction in the size of TESs can be obtained by using a suitable Phase Change Material (PCM), that is a medium that, at the typical operating temperature of the system, melts during the loading period and solidifies during the unloading operation. In solar plants, the use of hybrid water/PCM thermal energy storages can reduce the solar storage volume for a given solar fraction (how much of the solar radiation is useful for the heating/cooling purposes), or can increase the solar fraction for a given available volume [1]. As a further advantage, heat storage and delivery normally occur over a fairly narrow temperature range (the transition zone) [2].

A large number of PCMs (organic, inorganic, and eutectic) are available in any required temperature range [3]-[5]. As a matter of fact, due to their generally very low thermal conductivity (in the order of 0.2 W m^{-1} K^{-1}), the slowness of the loading or unloading of PCM storages is sometimes the most serious limitation to their use. Open-cell metal foams (a stochastic distribution of interconnected pores almost homogenous in size and shape) are a useful way to enhance the heat transfer performance as they feature high heat transfer area per unit of volume and high thermal conductivity. Mancin et al. [6] carried out some experiments measuring the improvement of the heat transfer by a metal foam during the solid–liquid phase change process of different paraffin waxes. More recently, Lazzarin et al. have conducted an extensive campaign measuring the temperature distribution and loading and unloading times of hybrid water PCM TES with and without aluminum (Al) foams [7]-[10].

The integration of PCM systems into commercial programs has been proposed in literature [11]. For the use in Trnsys [12], the type 860 has been developed to simulate water storage tanks including PCM modules (vertical cylinders, plates, or spherical beds) [13]. It is based on an enthalpy approach, considering conduction and convection into PCM as well as at the interface between PCM and water. A good agreement between numerical and experimental data has been obtained [14]. Recently, the authors simulated the use of Al foams to improve the heat transfer capabilities of paraffin waxes in hybrid water TESs based on Trnsys type 860 [15] [16]. Nevertheless, there is still a lack in literature of research that integrate PCM with metal foams in order to include hybrid water–PCM TES in dynamic thermo-energetic simulations for energy and economic evaluation of a solar heating/cooling and multi-source heat pump plant. Lazzarin et al. [17] have conducted a similar study, but it is limited to the comparison between sensible vs. PCM TES.

This paper reports a study of a dual source (solar thermal and ground) absorption heat pump system with three thermal storage tanks: the first producing hot water for heating, the second for domestic hot water (DHW), and the third producing cold water for cooling. The solar thermal energy is used directly for DHW and for heating, and it is also used as heat source for the heat pump, or to regenerate the ground when the system operates for summer air conditioning. In this case, condensation heat from the absorption chiller can be usefully directed to the post-heating coils of the air handling units, or to regenerate the ground as well. Annual simulations by the dynamic simulation software Trnsys are carried out based on an existing building that will be retrofitted during 2020 to become a nearly zero energy building (NZEB). An optimization of the solar and ground field designs from both energy and economic point of view is firstly performed. Subsequently, the energy performance of the plant is evaluated by considering different cases: all the three tanks modeled as sensible (water) storage, or one of the tanks modeled as PCM storage, or as enhanced PCM with metal foam. In the first part of the paper, the Trnsys type 860 is validated against some data collected during experimental tests.

Materials and Methods

PCM–Water Hybrid Thermal Storage: dynamic simulation model and experimental assessment

The simulation model developed in Trnsys based on type 860 proposed by Bony and Citherlet [13] to simulate water storage tanks including PCM modules (vertical cylinders, plates, or spheres bed) has been already described and validated with experimental data [10], [16]. Here, for the sake of brevity, only the main aspects of the analysis and validation are reported and discussed.

The tank is modeled to be made of stainless steel, 700 mm height, 350 mm diameter, 1 mm thick, water inlet at 700 mm height, and outlet at the bottom base, in order to validate it with previously measured experimental data. The tank is vertically divided into 35 water nodes (derivatives) and 30 PCM nodes, so axial nodes are 2 cm apart each other (Figure 1a).

The simulations are made at an imposed inlet temperature in order to make them comparable to the experimental tests. This condition is obtained by fixing tank inlet water flow rate and temperature at 500 L h^{-1} and 50 °C, respectively. Type 860 is set up with many parameters, among those:

- the temperature–enthalpy characteristic of the PCM Figure 1b reports the curve of the paraffin wax considered in the simulations);
- type and dimensions of the encapsulation: the PCM is considered inserted into two Al tubes (height 600 mm, inner diameter 48.6 mm, outer diameter 50.8 mm). One tube is supposed to be filled with the PCM, the other one with the PCM embedded in the Al-foam;
- values of solid and liquid thermal conductivity, specific heat capacity, and latent heat of fusion of the PCM as described in Table 1;
- the hysteresis parameter of type 860 is set up at 2.5 °C.

As type 860 cannot directly simulate metal foams inside the PCM encapsulation, the parameters related to radial and axial thermal conductivity of PCM in the liquid phase are simulated by the simplified model by Wang et al. [18]. An apparent thermal conductivity of paraffin/Al foam composite phase change material has been estimated as the equivalent thermal conductivity of an ideal homogeneous material exchanging the same heat as the real paraffin/Al foam composite.

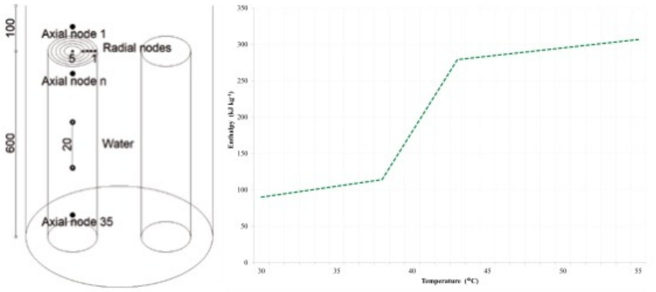

Figure 1 – (a) Schematic of the simulated system (not in scale, in millimeters); (b) enthalpy–temperature curve for the paraffin used in the simulations for type validation

Figura 1 – (a) Schema del sistema di accumulo simulato (disegno non in scala); (b) curva entalpia-temperatura della paraffina utilizzata nelle simulazioni per la validazione della type

Table 1 – **Main thermo-physical properties of the paraffin RT40**

Tabella 1 – Principali proprietà termofisiche della paraffina RT40

Phase Change Temperature (range) (°C)	Density (solid) (kg m^{-3})	Density (liquid) (kg m^{-3})	Latent Heat Capacity (kJ kg^{-1})	Specific Heat Capacity (solid) (kJ kg^{-1} K^{-1})	Specific Heat Capacity (liquid) (kJ kg^{-1} K^{-1})	Thermal Conductivity (W m^{-1} K^{-1})	Volume Expansion (%)
38–43	880	760	165	3.00	2.30	0.21	12.5

The series–parallel model of metal material and filler material is based on the thermal conductivity of the Al foam alloy (170 W m^{-1} K^{-1}) and that of the paraffin (0.21 W m^{-1} K^{-1}). As such, for porosity fixed at 0.90, 0.93, and 0.95 according to the experiment carried out by Lazzarin et al. [9], [10], the apparent thermal conductivity for the composite PCM in the liquid phase is 17.2, 12.1, and 8.70 W m^{-1} K^{-1}, respectively. Instead, the thermal conductivity of the composite PCM in the solid phase is fixed to be the same as the PCM (0.21 W m^{-1} K^{-1}). The experimental test rig and the comparison between simulation and experimental data have been extensively described in previous works of the authors [7]-[10] whose the reader can refer for the complete information.

Building Retrofitting and Thermal Loads Calculation

The building is part of an old (completed in 1960) high school building of Feltre, situated in the northern Italy. The gym and the laboratories will be retrofitted in order to become a NZEB [19]. The main part of the retrofitted building is a large gym (33 m × 25 m × 8.40 m, expanding on two levels). Changing rooms, bathrooms with toilet and showers, and technical rooms are located on the ground floor; an office, a small gym, and a bar are on the first floor. On the second floor, six laboratories will be retrofitted and made newly available (Figure 2).

The building has a total floor area of 2435 m², an outward surface area of 2505 m², and an enclosed gross heated volume of 11,060 m³. Based on the Trnsys 17 dynamic simulation, each thermal zone of the building is defined by means of scheduling the presence of people, type of activity, lighting and other internal gains, and air temperature set points. The HVAC system provides ventilation (by two air handling units, AHU), space heating and cooling, and DHW production. Figure 3 reports the heating, cooling, and DHW monthly energy needs calculated with a 0.25 h simulation time step.

The maximum cooling load (21.6 kW) occurs at the beginning of June, when the school is still fully operating, that is, it is open to students and professors, and gyms are open to extracurricular activities as well. The maximum heating load (–44.6 kW) occurs in the second half of January. However, even during summer months, post heating ventilation requires some heat. During the heating season, ventilation needs are prevailing with respect to heating needs; this is a consequence of the very high thermal insulation of the retrofitted building and of the minimization of thermal bridges. Moreover, DHW needs (2000 L per day at 45 °C) are a large quota of the total heat request.

Figure 2 – **The retrofitting intervention: building as is (left) and post-intervention (right)**

Figura 2 – Intervento di ristrutturazione: edificio nelle condizioni attuali (sinistra) e dopo intervento (destra)

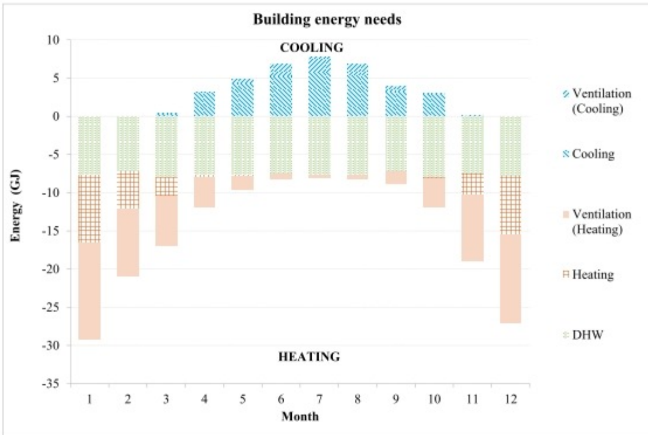

Figure 3 – **Monthly energy needs in terms of heating, cooling, ventilation (hot and cold coils of air handling units), and domestic hot water**

Figura 3 – Fabbisogni energetici mensili in termini di riscaldamento, raffrescamento, ventilazione (batterie di riscaldamento e raffrescamento delle unità trattamento aria) e acqua calda sanitaria

Table 2 – **Main technical characteristics of the absorption heat pump/chiller Robur GAHP-WS [20]**

Tabella 2 – Principali caratteristiche tecniche della pompa di calore/chiller ad assorbimento Robur GAHP-WS [20]

Operating as a Heat Pump	
Gas Utilization Efficiency (GUE)	174%
Heating power (condenser) (kW)	43.9
Heat source power (evaporator) (kW)	18.7
Operating Producing Useful Heating and Cooling	
Total efficiency index	248%
Operating as a Chiller	
Cooling power (evaporator) (kW)	18.7
Heating power (condenser) (kW)	43.9
Thermal power burner (kW)	25.2
Electric power (kW)	0.41

Table 3 – **Main technical characteristics of the solar collectors [21]**

Tabella 3 – Principali caratteristiche tecniche del collettore solare termico [21]

	Evacuated Tube	Flat Plate
Absorption area (m²)	2.55	1.84
η0 (@ 1000 W m^{-2})	72.10%	78.50%
a1 (W m^{-2} K^{-1})	1.051	3.594
a2 (W m^{-2} K^{-2})	0.004	0.014
IAM (50°)	1.09	0.94

The HVAC Plant

Through dynamic simulation using the Trnsys environment, different solutions are evaluated with respect to the HVAC system. A gas-fired absorption heat pump system is proposed to fulfill the needs of the building, utilizing ground and solar energy as cold source. The selected model has a modulating natural gas burner and stainless steel condensation heat recovery system, and it is able to produce alternatively or simultaneously hot water (until 65 °C) and cold water (until 3 °C) (Table 2).

A reduced functional diagram of the plant is shown in Figure 3. The HVAC system in the large gym provides space heating by means of a radiant floor, and space cooling by air conditioner units, while ventilation is realized by means of AHU (6600 $m^3 h^{-1}$) serving a single-duct system. The other spaces (small gym, bar, laboratories, and offices) are heated and cooled by fan coils, whereas toilets are heated only (by radiators), and laboratories are served also by an independent AHU (7000 $m^3 h^{-1}$) for ventilation. The two AHUs are equipped with heating and cooling coils, served by hot and cold main collectors in the central plant.

The thermal source for the heat pump can be either the ground or solar collectors. The former is set up by *n*x100 m in a row vertical tube U heat exchangers with an outer diameter of 32 mm and a thickness of 2.9 mm (*n* = 2-3-4 as a function of the solar field area as described in next section). Evacuated tube and flat plate collectors are considered in the simulation (Table 3). Solar collectors first serve the DHW tank, then the hot tank (for direct heating), and finally regenerate the ground.

The laboratories AHU is scheduled to work from 8 a.m. to 6 p.m. from Monday to Friday, and that of the large gym from 8 a.m. to 6 p.m. every day. The solar system is activated whenever the measured global solar radiation on the plane of collectors (tilt 18°, orientation South-East) exceeds a threshold radiation (100 W m^{-2}). Solar energy is always first directed to the DHW Tank, and successively to the Hot Tank. When the two tanks exceed the set point temperature (43 °C and 48 °C respectively) and the solar circuit outlet fluid temperature is above 15 °C, the flow is directed to the ground field to regenerate it. In this case, when the absorption machine is operating as a heat pump (heating season), the heat pump evaporator is supplemented by the solar section when its outlet temperature is lower than 30 °C. The DHW Tank is first served by solar energy. If solar energy is not enough, thermal energy is provided by the Hot Tank. The Hot Tank is fed by the solar circuit, and by the HP condenser. In both tanks, an electric auxiliary heater is present. The absorption HP/chiller is activated once the Hot/Cold Tank temperature falls below/above the given set points (48 °C and 7 °C respectively).

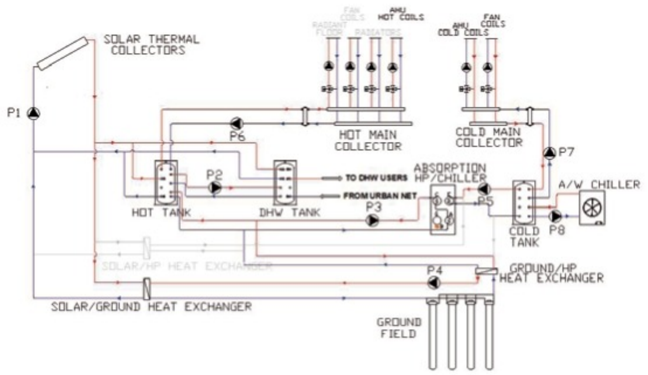

Figure 4 – Simplified functional diagram of the HVAC plant. The main circuits (ground, solar, tanks, hot and cold collectors) are shown (in grey the part of the plant operating during heating season only)

FIgura 4 – Schema funzionale semplificato dell'impianto HVAC. Sono disegnati i principali circuiti (terreno, solare, serbatoi, collettori caldo e freddo) (in grigio la parte dell'impianto in funzione solamente durante la stagione del riscaldamento)

Table 4 – Alternatives (all based on alternative A3 of Table 6) simulated with different storage tank configurations

Tabella 4 – Alternative simulate con le diverse configurazioni di serbatoi (tutte basate sull'alternativa A3 di Tabella 6)

Alternative	Hot Tank	DHW Tank	Cold Tank
B1≡A3	Sensible (water)	Sensible (water)	Sensible (water)
B2	Enhanced PCM	Sensible (water)	Sensible (water)
B3	PCM	Sensible (water)	Sensible (water)
B4	Sensible (water)	Enhanced PCM	Sensible (water)
B5	Sensible (water)	PCM	Sensible (water)
B6	Sensible (water)	Sensible (water)	Enhanced PCM
B7	Sensible (water)	Sensible (water)	PCM

Setting Parameters of Type 860

In the present study, seven alternatives are considered concerning the configuration of the three thermal storage tanks (Table 4) due to the limit of type 860 (it can be used only once in a Trnsys project, so no configurations with two PCM storage tanks can be simulated).

Table 5 reports the values of the main parameters of type 860. The dimensions of the tanks refer to real data from suppliers. The thickness of PCM tubes is supposed to be negligible. In order to avoid the risk of laminar water flow around the tubes, their number is fixed allowing a suitable space between each other. The commercial paraffin waxes Rubitherm® RT47, RT42, and RT7 are used for the hot, DHW, and cold tanks respectively, with phase change temperatures centered in the most suitable range for each tank. The porosity of enhanced Al-foam PCM is fixed at 0.93, the apparent thermal conductivity in liquid phase is 12.1 W $m^{-1} K^{-1}$. At ambient temperature, each tube contains 3.63 kg and 3.35 kg for the PCM and enhanced PCM case respectively.

Table 5 – Main parameters of type 860 simulating the three hybrid water–PCM thermal storage tanks as described in Figure 4

Tabella 5 – Principali parametri della type 860 che simula i tre serbatoi di accumulo ibridi acqua-PCM come descritto in Figura 4

	DHW Tank	Hot Tank	Cold Tank
Tank diameter (mm)	1318	1318	841
Tank height (mm)	2200	2200	1800
Tubes diameter (mm)	50	50	50
Tube height (mm)	2100	2100	1700
Number of tubes	216	216	85
PCM radial liquid conductivity (W $m^{-1} K^{-1}$)	0.21	0.21	0.21
Enhanced PCM radial liquid conductivity (W $m^{-1} K^{-1}$)	12.1	12.1	12.1

AiCARR Journal / Vol 62, n. 3, 56 - 63, 2020

Table 6 – **Different alternatives simulated with solar field, ground boreholes, and storage tank dimensions (all considering sensible (water) storage)**

Tabella 6 – Alternative simulate con dimensioni del campo solare, del terreno e degli accumuli (considerati come accumuli sensibili (acqua))

Alternative	Type of Collector	Solar Field Area (m²)—Ground Boreholes Depth (m)	DHW Tank (L)	Hot Tank (L)	Cold Tank (L)
A1	-	0	1500	1500	1000
A2	Evacuated tube	20–400	1500	2000	1000
A3	Evacuated tube	40–300	3000	3000	1000
A4	Evacuated tube	60–200	3000	5000	1000
A5	Flat plate	50–300	3000	5000	1000

Results and Discussion

In the first step, energy analysis results are reported in terms of monthly energy balances considering the three tanks (hot, cold and DHW) as sensible (water) storages with the aim of determining the size of the solar and ground fields of the most viable mixed solution (Table 6). Successively, annual energy performance results are reported comparing different alternatives among sensible, PCM, and enhanced PCM systems (Table 4) in order to determine the best tanks configuration.

Monthly Energy Analysis

Next Figure 5 – Figure 8 refer to A3 case (40 m² evacuated tube—300 m ground probes). As a result of the balance of solar radiation impinging the collectors, hot water for heating (green in Figure 5) and sanitary uses (red) is provided during the whole year, whereas the quota directed to regenerate the ground is mainly in summer time (light blue). The quota of solar energy directed to the HP evaporator is negligible (only alternative A5 features a significant value due to the lower thermal efficiency of the flat plate collectors in winter

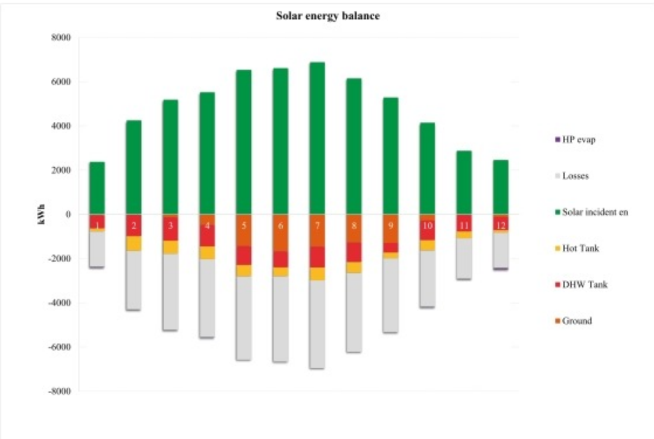

Figure 5 – **Solar energy balance for the A3 alternative**

Figura 5 – Bilancio dell'energia solare per l'alternativa A3

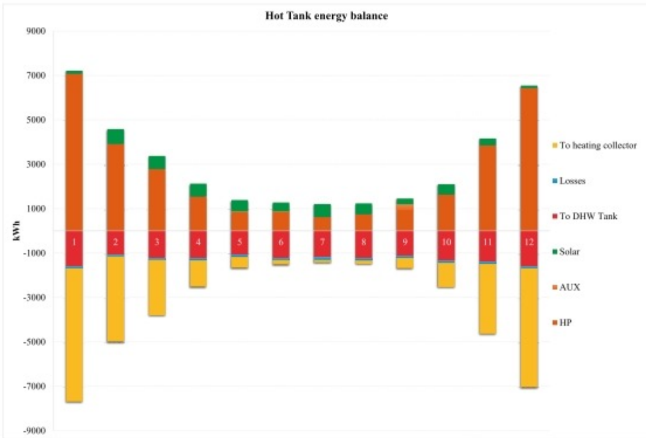

Figure 7 – **Energy balance for the Hot Tank for the A3 alternative**

Figura 7 – Bilancio energetico dell'Hot Tank per l'alternativa A3

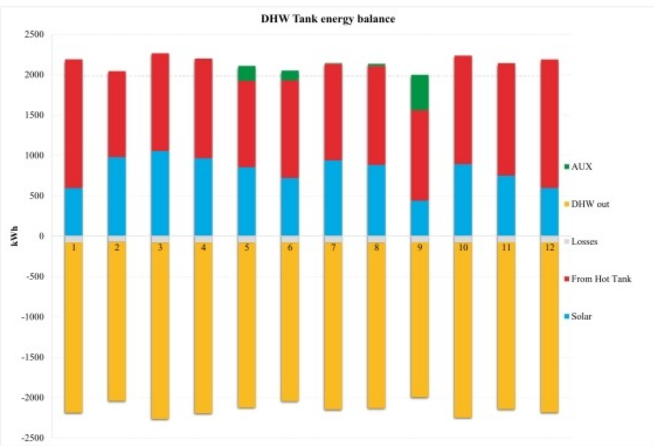

Figure 6 – **Energy balance for the DHW Tank for the A3 alternative**

Figura 6 – Bilancio energetico del DHW Tank per l'alternativa A3

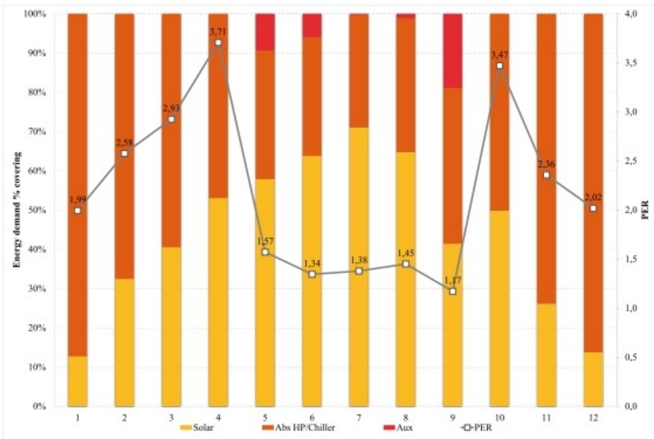

Figure 8 – **Energy demand percentage covering of different energy sources and the primary energy ratio (PER) (alternative A3)**

Figura 8 – Percentuali di copertura del fabbisogno richiesto da parte delle diverse sorgenti e rapporto di energia primario (PER) (alternativa A3) conditions with respect to the evacuated tube).

An appreciable contribution to DHW demand is by solar energy; furthermore, the Hot Tank contribution prevails mainly in the colder months (Figure 6 and Figure 7). The control logic of the absorption HP/chiller as above described allows to hardly limit the contribution of electric auxiliaries, present mainly during the summer or mid-season. In fact, in winter the absorption machine operates as HP, and it is controlled by the Hot Tank set point temperature (the DHW tank is also satisfied mainly by solar energy and the Hot Tank). During summer or mid-season, it operates as chiller controlled by the Cold Tank set point temperature: the heat recovered by the condenser is available only when it is on.

For the A3 alternative, the results are reported in Figure 8 in terms of primary energy ratio (PER); the percentages covering of different heat generators (solar collectors, absorption HP, and electric auxiliaries) are reported as well. PER is defined as the ratio between useful energy produced by the plant (energy from the three tanks to the main collectors in Figure 4) and the total no-renewable primary energy consumed (that is natural gas supplied to the absorption machine, and electricity to the electric auxiliaries of the Hot Tank and DHW Tank converted in primary energy by the factors $f_{p,nren}$ = 1.05 and 1.95 respectively according to Italian standard DM 26/06/2015). Figure 8 confirms that, during cold season, the heat pump covers the largest fraction of heating and DHW load, with a PER always greater than 1.94. Furthermore, the low GUE of the absorption machine in chiller mode (between 0.74 and 0.79), and the low contribution of the heat recovered by the chiller to the heating and DHW demand determine the lowest values of PER during hot season. Finally, the ground energy balance is positive for all the alternatives, that is, energy injected into the ground exceeds energy extracted.

Annual Energy and Economic Analysis

The annual PER is reported in Figure 9, also considering the electricity consumption by the circulation pumps (PER*). The latter is not negligible at all, mainly due to the pressure drops of the ground circuit. For example, for the A3 case the annual pump electricity consumption is around 1650 kWh: this is 3% of the total thermal and cooling useful energy, and around 11% of the total no-renewable primary energy supplied to the plant. Such a percentage is consistent with data found in previous authors' work in similar multi-source heat pump plants [22]-[24].

From the energy performance point of view, the best solution is A4 (PER = 2.12, PER* = 1.92), whereas A3 is in second place. A more comprehensive choice of the preferred alternative was done by considering the economic point of view [25] based on reasonable estimates of the equipment's investment cost, natural gas and electricity costs, and the value of the economic incentive ("Conto Energia Termico 2.0"). As a matter of fact, the most profitable solution results to be a multi-source HP plant with 40 m² of evacuated tube and 300 m boreholes (A3), that allows gains of around 40 k€ in 20 years.

Annual Energy Analysis for Determining the Best Storage Tanks Configuration

The final part of the study reports the assessment of the use of PCM and enhanced PCM hybrid storage tanks. In terms of no-renewable primary energy consumption and PER of the plant, B2 and B3 alternatives feature the best performance (Figure 10). Using PCM tubes in the DHW Tank is a viable solution because the use of solar energy for DHW production is increased by 19%, even though in the Hot Tank is decreased by 32% (Figure 11). Moreover, using PCM in the Hot

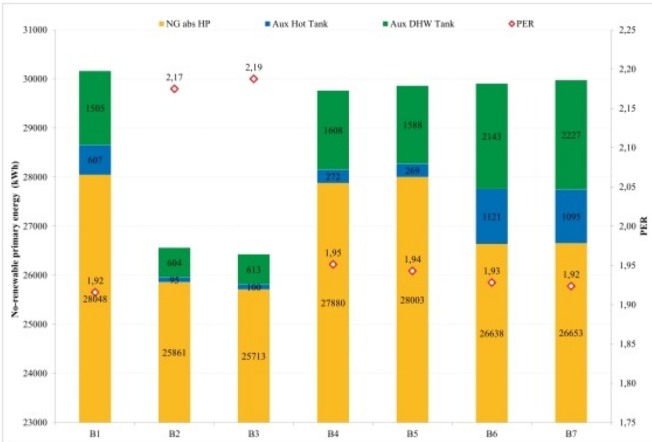

Figure 10 – No-renewable primary energy consumption and primary energy ratio for the different alternatives

Figura 10 – Consumo di energia primaria non rinnovabile e rapporto di energia primaria per le diverse alternative

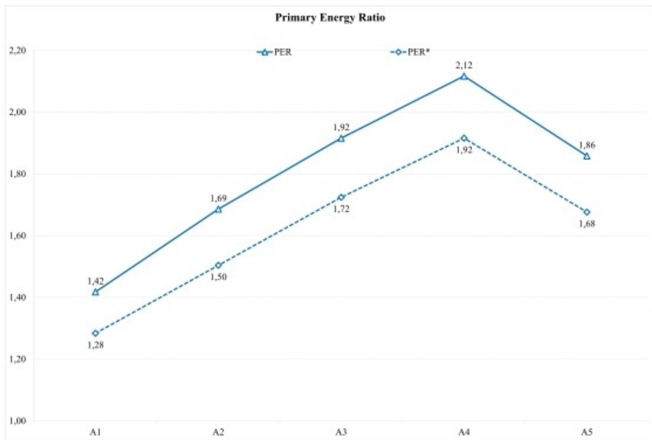

Figure 9 – PER (also considering the electricity consumption by the circulation pumps (PER*)) for the different alternatives

Figura 9 – PER (anche considerando il consumo di energia elettrica delle pompe (PER)) per le diverse alternative*

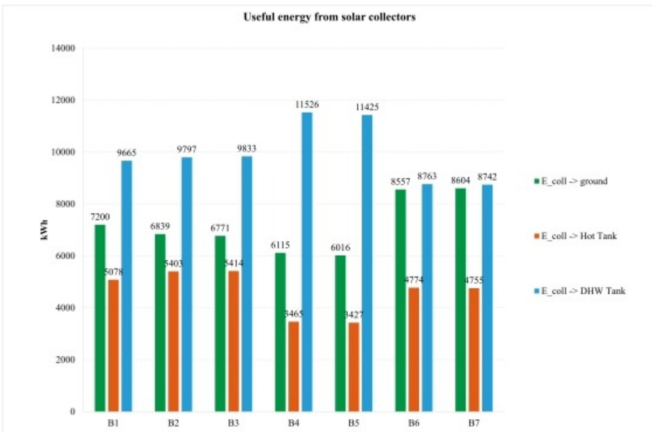

Figure 11 – Useful solar radiation from thermal collectors to ground, Hot Tank and DHW Tank

Figura 11 – Energia solare utile dai collettori verso il terreno, Hot Tank e DHW Tank

AiCARR Journal / Vol 62, n. 3, 56 - 63, 2020

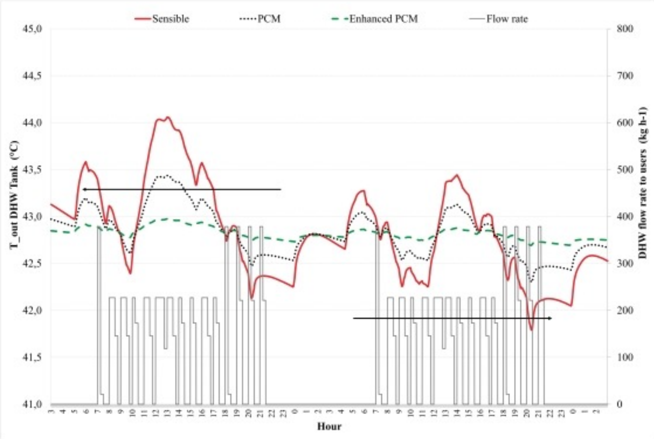

Figure 12 – Temperature and flow rate of water at the outlet of the DHW Tank in the case of sensible (water), PCM and enhanced PCM DHW Tank

Figura 12 – Temperatura e portata d'acqua all'uscita del DHW Tank nel caso di accumulo DHW Tank sensibile (acqua), PCM e PCM incentivato

Tank increases the use of solar energy for heating because 7% more energy can be stored in the tank. As a matter of fact, higher energy saving can be obtained using PCM tubes in the Hot Tank because the heat pump operates with a higher GUE due to lower temperature of hot water produced.

Even if the use of enhanced PCM does not allow appreciable energy savings with respect to PCM (Figure 10), an advantage of its use is a narrower temperature range of hot water at the outlet of the tank. This means that the heat stored inside the PCM is efficiently rejected to the water when the Al-foams are used. For example, Figure 12 reports the outlet temperature of the DHW Tank for two typical days in three cases: sensible (water), PCM, and enhanced PCM storage. The more constant temperature of hot water at the outlet of the tank when using enhanced PCM guarantees a higher level of service for the DHW produced.

Conclusions

A case study for energy and economic analysis of a multi-source (solar and ground) absorption heat pump plant for the heating and cooling is presented. As the operating temperature of the storage depends on the solar collectors' area, on the volume of the storage tanks, and on the kind and entity of the thermal loads, a transient simulation allows to define the size and the type (sensible or PCM or enhanced PCM) of the three thermal energy storage systems (for DHW production, for heating, and for cooling). 40 m² evacuated tube, 300 m ground probes, 3000 L Hot Tank and DHW Tank capacity (filled with PCM RT47), 1000 L Cold Tank capacity (sensible storage) is the best plant configuration from the energy point of view, featuring the highest PER and solar ratio. As a matter of fact, the mean operating temperature of the Hot Tank is near the melting temperature of the PCM for longer during the year. No additional advantage by using Al-foam enhanced PCM is yielded. Instead, a more constant hot water temperature is allowed, thus a higher level of service for the hot water produced is guaranteed. Due to the greater investment cost of PCM and enhanced PCM technologies with respect to sensible storage, their viability should be evaluated by a wider economic evaluation of the proposed study.

FUNDING

This research project was partially funded by: MIUR, Italy, PRIN 2017: "The energy FLEXibility of enhanced HEAT pumps for the next generation of sustainable buildings (FLEXHEAT)" (grant number 2017KAAECT).

ACKNOWLEDGEMENT

The authors would like to thank Lorenzo Zamboni and Alberto Matteazzi for supporting the simulations.

REFERENCES

[1] Medrano, M.; Yilmaz, M.O.; Nogués, M.; Martorell, I.; Roca, J.; Cabeza, L.F. Experimental evaluation of commercial heat exchangers for use as PCM thermal storage systems. Applied Energy 2009, 86, 2047–2055, doi.org/10.1016/j.apenergy.2009.01.014.

[2] Paris, J.; Falardeau, M.; Villeneuve, C. Thermal storage by latent heat: A viable option for energy conservation in buildings. Energy Sources 1993, 15, 85–93, doi.org/10.1080/00908319308909014.

[3] Agyenim, F.; Hewitt, N.; Eames, P.; Smyth, M. A review of materials, heat transfer and phase change problem formulation for latent heat thermal energy storage systems (LHTESS), Renewable & Sustainable Energy Reviews 2010, 14, 615-628, doi.org/10.1016/j.rser.2009.10.015.

[4] Du, K.; Calautit, J.; Wang, Z.; Wu, Y.; Liu, H. A review of the applications of phase change materials in cooling, heating and power generation in different temperature ranges. Applied Energy 2018, 220, 242–273, doi.org/10.1016/j.apenergy.2018.03.005.

[5] Jaguemont, J.; Omar, N.; Van den Bossche, P.; Mierlo, J. Phase-change materials (PCM) for automotive applications: A review. Applied Thermal Engineering 2018, 132, 308–320, doi.org/10.1016/j.applthermaleng.2017.12.097.

[6] Mancin, S.; Diani, A.; Doretti, L.; Hooman, K.; Rossetto, L. Experimental analysis of phase change phenomenon of paraffin waxes embedded in copper foams. Int. J. Therm. Sci. 2015, 90, 79–89, doi.org/10.1016/j.ijthermalsci.2014.11.023.

[7] Lazzarin, R.; Mancin, S.; Noro, M.; Righetti, G. Experiment Analysis of Aluminum Foams as heat transfer medium for PCM Thermal Storages, Refrigeration Science and Technology. In Proceedings of the 5th IIR International Conference on Thermophysical Properties and Transfer Processes of Refrigerants, Seoul, Korea, 23–26 April 2017; paper TP-0024, doi.org/10.18462/iir.tptpr.2017.0024.

[8] Lazzarin, R.; Mancin, S.; Noro, M.; Righetti, G. Porous media for advanced hybrid thermal energy storages, Refrigeration Science and Technology. In Proceedings of the 12th IIR Conference on Phase Change Materials and Slurries for Refrigeration and Air Conditioning, Orford, QC, Canada, 21–23 May 2018; pp. 379–386, ISBN 978-2-36215-025-8, ISSN: 0151-1637, doi.org/10.18462/iir.pcm.2018.0051.

[9] Lazzarin, R.; Mancin, S.; Noro, M.; Righetti, G. Hybrid PCM—Aluminium foams' thermal storages: An experimental study. Int. J. Low Carbon Technol. 2018, 13, 286–291, doi.org/10.1093/ijlct/cty030.

[10] Righetti G.; Lazzarin R.; Noro M.; Mancin S. Phase Change Materials embedded in porous matrices for hybrid thermal energy storages: Experimental results and modelling, International Journal of Refrigeration 2019, 106, 266-277, doi.org/10.1016/j.ijrefrig.2019.06.018.

[11] Castell, A.; Solé, C. Design of latent heat storage systems using phase change materials (PCMs). In Advances in Thermal Energy Storage Systems. Methods and Applications, Woodhead Publishing Series in Energy; Woodhead Publishing: Sawston, UK, 2015; pp. 285–305.

[12] Klein, S.A.; et al. 2010. TRNSYS 17: A Transient System Simulation Program, Solar Energy Laboratory, University of Wisconsin, Madison, USA. Available online: http://sel.me.wisc.edu/trnsys (accessed on 30 May 2020).

[13] Bony, J.; Citherlet, S. Extension of a TRNSYS model for latent heat storage with phase change materials used in solar water tank. In Proceedings of the ECOSTOCK 2006—10th International Conference on Thermal Energy Storage, Pomona, NJ, USA, 31 May–2 June 2006.

[14] Bony, J.; Citherlet, S. Numerical model and experimental validation of heat storage with phase change materials. Energy Build. 2007, 39, 1065–1072, doi.org/10.1016/j.enbuild.2006.10.017.

[15] Lazzarin, R.; Mancin, S.; Noro, M. Experiment for the evaluation of Aluminum foams for improving heat transfer in PCM thermal storages, Refrigeration Science and Technology. In Proceedings of the 11th IIR Conference on Phase Change Materials and Slurries for Refrigeration and Air Conditioning, Karlsruhe, Germany, 18–20 May 2016; pp. 122–131, ISBN 978-2-36215-015-9, ISSN 01511637, doi.org/1 0.18462/iir.pcm.2016.0016.

[16] Lazzarin, R.; Mancin, S.; Noro, M.; Righetti, G.; Zamboni, L. Simulation of the phase change process of paraffin waxes with and without Aluminum foams for advanced hybrid thermal energy storages, Refrigeration Science and Technology. In Proceedings of the 12th IIR Conference on Phase Change Materials and Slurries for Refrigeration and Air Conditioning, Orford, QC, Canada, 21–23 May 2018, pp. 256–264, ISBN: 978-2-36215-025-8, ISSN: 0151-1637, doi.org/10.18462/iir.pcm.2018.0035.

[17] Noro, M.; Lazzarin, R.; Busato, F. Solar cooling and heating plants: An energy and economic analysis of liquid sensible vs phase change material (PCM) heat storage. Int. J. Refrig. 2014, 39, 104–116, doi.org/10.1016/j.ijrefrig.2013.07.022.

[18] Wang, Z.; Zhang, Z.; Jia, L.; Yang, L. Paraffin and paraffin/Al foam composite phase change material heat storage experimental study based on thermal management of Li-ion battery. Appl. Therm. Eng. 2015, 78, 428–436, doi.org/10.1016/j.applthermaleng.2015.01.009.

[19] Lazzarin R.; Noro M. Photovoltaic/Thermal (PV/T) / ground dual source heat pump: optimum energy and economic sizing based on performance analysis, Energy and Buildings 2020, 211, 109800, doi.org/10.1016/j.enbuild.2020.109800.

[20] Robur S.p.A. Design manual 2017, Italy. 2017. Available online: http://www.robur.it (accessed on 12 August 2020).

[21] Kloben Industries S.r.l. Priced Catalogue 2017, Italy. 2017. Available online: hiip://www.kloben.it (accessed on 12 August 2020).

[22] Busato, F.; Lazzarin, R.; Noro, M. Two years of recorded data for a multisource heat pump system: A performance analysis. Appl. Therm. Eng. 2013a, 57, 39-47, doi.org/10.1016/j.applthermaleng.2013.03.053.

[23] Busato, F.; Lazzarin, R.; Noro, M. Multisource heat pump system from design to operation: The case study of a new school building. Int. J. Low Carbon Technol. 2013b, 8, 88–94, doi.org/10.1093/ijlct/ctt002.

[24] Busato, F.; Lazzarin, R.; Noro, M. Ground or solar source heat pump systems for space heating: Which is better? Energetic assessment based on a case history. Energy Build. 2015, 102, 347–356, doi.org/10.1016/j.enbuild.2015.05.053.

[25] Lazzarin, R.; Noro, M.; Righetti, G.; Mancin, S. Application of Hybrid PCM Thermal Energy Storages with and without Al Foams in Solar Heating/Cooling and Ground Source Absorption Heat Pump Plant: An Energy and Economic Analysis, Applied Sciences 2019, 9(5), 1007, doi.org/10.3390/app9051007.